



## Groundwaters hydro-geochemical characterization of the Tagharist basin (northern region of Khenchela, south-eastern Algeria)

Sekkiou Salah Eddine<sup>a,\*</sup>, Houha Belgacem<sup>b</sup>

<sup>a</sup>Department of Ecology and Environment, Biotechnological Laboratory of Water, Environment and Health, Abbes Laghrour University, BP 40000 Khenchela, Algeria, Tel. +213 0670230911; email: salaseovic907@gmail.com

<sup>b</sup>Biotechnological Laboratory of Water, Environment and Health, Abbes Laghrour University, BP 40000 Khenchela, Algeria, Tel. +213 0665627684; email: bhouha@yahoo.fr

Received 12 December 2017; Accepted 15 November 2018

---

### ABSTRACT

In order to evaluate the physicochemical quality of groundwater in the Tagharist Wadi basin, which is part of the semi-arid regions of south-eastern Algeria, and to identify the mechanisms resulting in the mineralization of groundwater, physicochemical analyses have been carried out on 34 water samples of Plio-Quaternary aquifer. The study area is a mountainous zone consisted of a certain number of secondary ranges, which form the relief of the Aures massif. The stratigraphic series belong to secondary, with, at the top, Miocene sandstones of limited extension in depth, which rest in discordance on the limestones and marl-limestones of Cretaceous; this set is covered by Quaternary consisted of a low proportion of red clay, pebbles, gravels, and coarse sand; these alluvia are of calcareous, predominant, and sandy nature. The result obtained showed that the bicarbonate-calcium facies dominates (94% of wells), and it originates from carbonate formations going along the water table; the rest (6% of wells) are of sodium-bicarbonate facies. Electrical conductivity of water has an average value of 974.75  $\mu\text{S}/\text{cm}$ . It is to be noted that the borehole P4 shows a high electrical conductivity, probably due to irrigation return flow, the salinity of which would be accentuated by evaporation and dissolution of some evaporitic inclusions. Saturation index shows that groundwater of the study area is undersaturated with respect to gypsum, halite, and anhydrite. In contrast, carbonate-calcium formations (calcite and aragonite) tend to be balanced. The descriptive analysis shows that water salinity is very variable from place to place and increases in the water flow direction, impacted by water-rock interaction, mineral dissolution and precipitation, base exchange, and anthropogenic activity.

*Keywords:* Groundwater; Plio-Quaternary; Salinity; Base exchange; Tagharist basin; Algeria

---

### 1. Introduction

The water chemical composition of the wells and the springs is mainly acquired during its crossing of the soil and its residence in the reservoir. Water in contact with the host rock acquires a mineral load typical of the crossed rocks. The elements existing in solution therein are informative of the crossed aquifer nature.

The Tagharist Wadi constitutes the only water reservoir of the mountainous area, characterized by a steep relief. Arboriculture (apple and apricot trees) has a high level growth in terms of farming development, with the emergence of new fruits packaging industry, which has contributed to the stabilization of rural populations, accompanied by solid and liquid discharge. The water tables of the upper plains, being subject to pressure due to the exploitation of

---

\* Corresponding author.

their water, undergo a degradation of their chemical quality, caused by natural processes, as well as by anthropogenic activity. Our objective is to contribute to the understanding of the mineralization process of groundwater in these areas, using tools such as major and minor elements.

We have used the statistical and chemical tools approach to better discriminate the processes responsible for the mineralization acquisition of the Tagharist Wadi valley water. It is then important to rank the processes resulting in the modification of the water chemical composition and that induced their degradation.

## 2. Materials and methods

### 2.1. Study area

The Tagharist Wadi basin is part of the semi-arid areas of south-eastern Algeria, located about 40 km from the chief town of the Khenchela province between 35°40' and 35°50' of northern latitude, and between 6°50' and 6°60' of eastern longitude. The basin is limited to the south by Djebel Chelia, and to the north by the Remila plain (Fig. 1).

The climate of the study area is semi-arid, with an annual mean rainfall of 392 mm, and a mean annual temperature of 15.8°C.

The study area is a mountainous zone consisted of a certain number of secondary ranges, which form the relief of the Aures massif. The stratigraphic series belong to secondary, with, at the top, Miocene sandstones of limited extension in depth, which rest in discordance on the limestones and marl-limestones of Cretaceous; this set is covered by Quaternary consisted of a low proportion of red clay, pebbles, gravels, and coarse sand; these alluvia are of calcareous, predominant, and sandy nature. Triassic blunting is visible in Djebel Aidel and Djebel El-Krouma in the Khenchela area [1]. The ancient formations start at the top with Miocene sandstones which rest in discordance on the Cretaceous

formations; this is an alternation of sandstones bank and grey clay having a thickness of 400 m that dips in depth, but it is of limited extension. Cretaceous is represented by thick series of grey marl, which are homogeneous enough and finely jointed and fractured in places. The stratification is underlined by marl-limestone fine banks of a very light color. A large calcareous dolomitic strip, attributed to Santonian develops. Turonian presents itself as an alternation of thick grey marls, encompassing calcareous banks having a thickness of 500–600 m. Basal Turonian is consisted of marls having a thickness of 300–400 m. Lower Cretaceous, represented by Albo-Aptian, is a succession of marls and limestone having a thickness of 600 m.

The geological profile of the crossed terrains (Fig. 2), following an NW-SE path, indicates a succession of terrains of different natures, dipping about 45° downstream. The limestone outcrops and Miocene sandstone are the most visible and dominant, topped by a sediment cover of Quaternary.

Hydrologically, the area has two types of aquifer: multi-layer aquifers of sedimentary basin consisted of Plio-Quaternary aquifers, and aquifers of carbonate fissured formations of Cretaceous.

### 2.2. Sampling and analysis

In order to study the quality of groundwater of the Tagharist Wadi basin, the origin of salinity and its spatial evolution, we have conducted a study of water chemistry.

A complete analysis of chemical major elements and a couple of trace elements have been carried out on 34 samples of water collected in June 2016. Electrical conductivity, water temperature, and pH have been measured in the field by means of multi-parameter of type « CONSORT C931 », Chemical elements have been analyzed at the laboratory of environmental analyses and chemical trials on materials, cations by flame atomic absorption, anions, and trace elements have been dosed by titrimetry and spectrophotometry

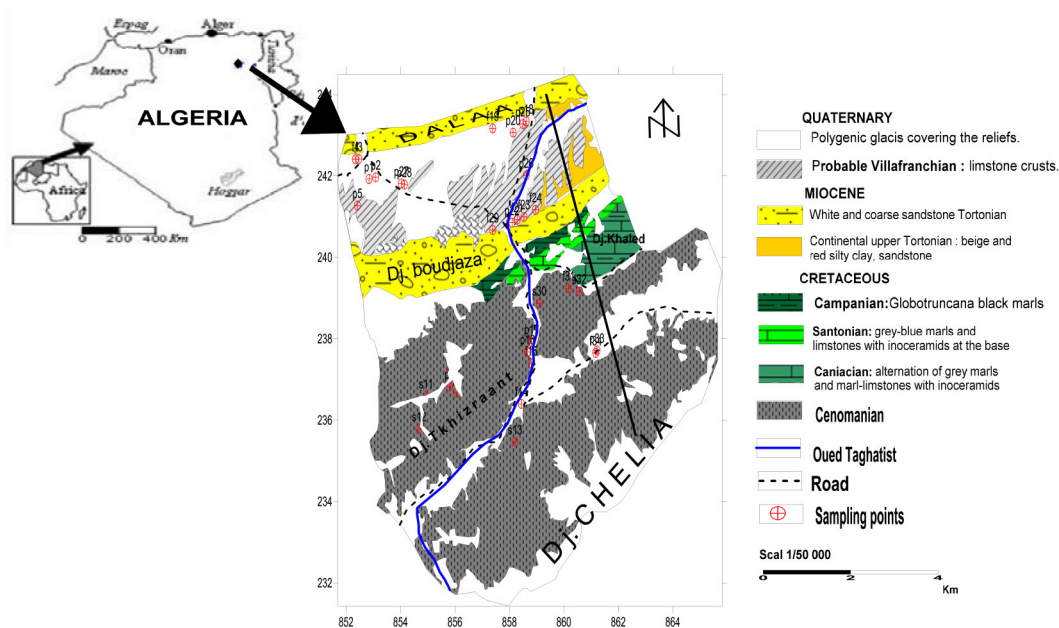


Fig. 1. Geological map of the study area (according to geological map of Touffana).

HACH-(DR2000) in LACILAP Laboratory (Ain M'lila, Algeria, May 2016). The results processing has been carried out using the software diagrams of the University of Avignon (France).

### 3. Results and discussion

#### 3.1. Chemical facies

Chemical analyses (Table 1) show that groundwater is low to moderately mineralized, with electrical conductivity values oscillating between 400 and 2,174  $\mu\text{S}/\text{cm}$ , except for borehole 4 which displays a value of 3,948  $\mu\text{S}/\text{cm}$ . The representation of major elements concentrations on Piper diagram [2] (Fig. 3) shows that this groundwater is generally

characterized by a chemical facies where bicarbonates, sulfates, calcium, and sodium are dominant. In detail, this water is distributed between the following poles:

- bicarbonate-calcium facies (94% of wells) originates from carbonate formations going along the water table
- bicarbonate-sodium facies (6% of wells)

The observation of the piezometric map morphology [1] allows seeing that the groundwater flow occurs generally following a south-west direction toward the north-east (Fig. 4).

The drainage axis of groundwater coincides sensitively with the course of the Boulefraï Wadi, which drains surface water.

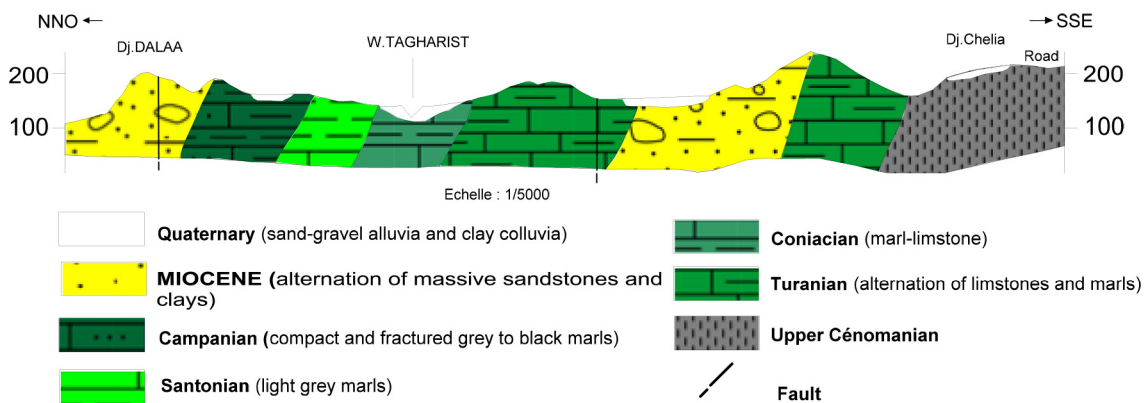


Fig. 2. The geological profile of the crossed terrains (ANB March 2006).

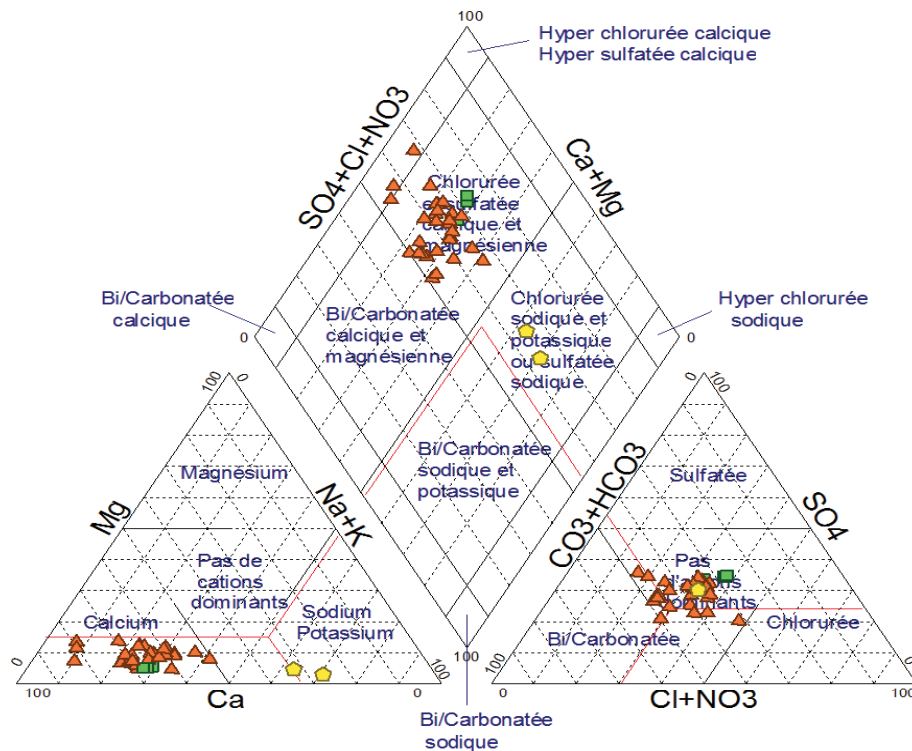


Fig. 3. Piper diagram for all water of the Tagharist Wadi basin.

Table 1  
Results of groundwaters physicochemical analyses of the Tagharist Wadi basin (June 2016)

Point	CE ( $\mu\text{S/cm}$ )	pH	TDS (mg/L)	Ca (mg/L)	Mg (mg/L)	Na (mg/L)	K (mg/L)	HCO <sub>3</sub> (mg/L)	Cl (mg/L)	SO <sub>4</sub> (mg/L)	NO <sub>3</sub> (mg/L)	NO <sub>2</sub> (mg/L)	Saturation index		Dolomite	Gypsum	Halite	
													Anhydrite	Aragonite				
P1	1,355	7.82	710	115.3	11.65	71.2	5.3	285.2	66.54	122.4	32.36	0.012	-1.62	-0.17	-0.02	-0.7	-1.4	-6.92
P2	1,770	7.70	893	142.5	13.25	88.3	6.5	354.3	92.33	167.8	28.55	0.01	-1.44	-0.02	0.13	-0.43	-1.22	-6.69
P3	1,811	7.6	912	158.3	14.55	75.4	7.2	360.0	98.31	171.3	26.88	0.003	-1.4	0.03	0.17	-0.34	-1.18	-6.74
P4	3,948	7.31	2,022	396.6	16.37	165.7	11.5	796.3	233.4	366.8	25.12	0.012	-0.9	0.64	0.79	0.54	-0.68	-6.06
P5	896	7.70	463	88.54	4.55	43.5	2.8	128.5	48.34	102.2	45.67	0.013	-1.73	-0.58	-0.44	-1.83	-1.51	-7.26
P6	983	7.57	474	91.27	4.98	29.8	3.6	145.7	52.47	106.5	41.13	0.015	-1.7	-0.52	-0.38	-1.67	-1.48	-7.39
P7	967	7.37	462	91.77	5.05	28.4	4.6	141.4	49.66	99.03	42.12	0.011	-1.73	-0.53	-0.38	-1.68	-1.51	-7.43
P8	923	7.51	468	85.44	7.64	40.3	5	139.9	47.38	98.13	44.88	0.01	-1.76	-0.56	-0.42	-1.54	-1.54	-7.3
P9	1,069	7.43	511	103.6	8.32	36.2	4.9	145.2	55.27	111.5	46.39	0.016	-1.65	-0.48	-0.33	-1.42	-1.43	-7.28
P10	1,441	8.00	692	62.32	5.33	135	6.3	204.6	89.32	138.3	50.51	0.039	-1.78	-0.57	-0.43	-1.58	-1.56	-6.51
P11	787	7.29	385	71.77	8.18	27.3	3.1	122.2	41.27	78.25	33.45	0.009	-1.9	-0.68	-0.53	-1.66	-1.68	-7.52
P12	632	7.34	312	55.39	6.31	22.1	3.4	102.3	32.65	58.95	31.12	0.011	-2.09	-0.84	-0.7	-1.99	-1.87	-7.71
P13	433	7.98	203	48.65	2.55	5.6	1.9	76.31	19.37	32.27	16.37	0.012	-2.35	-0.99	-0.84	-2.62	-2.13	-8.52
P14	619	7.37	281	61.24	6.32	5.2	2.2	80.21	32.54	62.36	31.24	0.014	-2.02	-0.9	-0.76	-2.15	-1.8	-8.34
P15	543	7.61	262	50.22	6.02	13.5	1.3	77.32	24.56	60.24	29.35	0.009	-2.1	-0.99	-0.85	-2.28	-1.88	-8.04
P16	538	7.58	261	46.34	5.12	17.9	1.1	81.29	21.33	55.36	33.4	0.007	-2.17	-1	-0.86	-2.33	-1.95	-7.98
P17	552	7.98	269	47.56	2.81	16.5	2.4	111.1	27.11	36.54	19.32	0.011	-2.32	-0.85	-0.7	-2.29	-2.1	-7.91
P18	1,173	7.70	576	108.9	10.13	47.2	8.6	163.5	69.32	119.2	51.27	0.031	-1.62	-0.42	-0.27	-1.23	-1.4	-7.08
P19	544	7.73	260	46.36	2.11	29.34	1.1	86.66	30.21	42.32	21.27	0.009	-2.27	-0.97	-0.82	-2.64	-2.05	-7.61
P20	2,174	7.64	1,079	244.7	21.26	26.3	5.6	399.5	115.8	238.2	27.95	0.006	-1.15	0.23	0.37	0.03	-0.93	-7.14
P21	704	7.71	347	65.23	4.56	29.2	3.5	106.3	52.44	65.21	21.22	0.011	-2	-0.76	-0.62	-2.05	-1.78	-7.39
P22	400	8.41	198	39.66	3.2	12.3	2.1	69.32	26.35	30.08	16.35	0.003	-2.45	-1.11	-0.97	-2.68	-2.23	-8.04
P23	494	7.69	245	42.02	4.28	22.6	2.6	77.07	28.92	36.55	31.47	0.016	-2.37	-1.06	-0.91	-2.47	-2.15	-7.74
P24	591	7.94	296	47.47	5.63	25.2	2.9	79.03	31.52	39.21	66.31	0.008	-2.31	-1	-0.86	-2.3	-2.09	-7.66
P25	1,691	7.55	849	169.3	8.66	68.4	5.6	231.4	45.67	188.9	33.54	0.01	-1.32	0.01	0.16	-0.63	-1.1	-7.11
P26	716	7.89	340	55.39	5.1	29.4	4	112.0	35.96	71.99	27.39	0.011	-2.01	-0.81	-0.67	-2.02	-1.79	-7.54
P27	1,983	7.98	987	195.2	8.85	90	7.2	244.7	163.4	234.7	44.21	0.013	-1.21	-0.07	0.08	-0.85	-0.99	-6.45
P28	2,063	7.772	1,031	200.3	8.92	88.3	6.9	251.5	177.0	252.0	46.38	0.017	-1.18	-0.05	0.09	-0.82	-0.96	-6.42
P29	644	7.786	319	45.68	4.25	41.2	3.1	89.73	29.37	64.33	42.31	0.016	-2.12	-0.98	-0.84	-2.36	-1.9	-7.48
P30	561	7.586	263	44.35	3.56	22.7	2.2	80.27	22.35	52.23	35.36	0.009	-2.2	-1.02	-0.88	-2.51	-1.98	-7.86
P31	818	7.34	396	61.25	7.05	45.8	5.3	112.3	42.01	73.11	49.37	0.014	-1.99	-0.78	-0.63	-1.86	-1.77	-7.29
P32	732	7.308	345	58.63	6.55	29.9	4.8	122.3	28.34	66.37	28.14	0.008	-2.03	-0.75	-0.6	-1.82	-1.81	-7.64
P33	541	7.617	254	49.66	3.12	17.3	3.6	70.33	2.55	50.24	32.58	0.011	-2.17	-0.95	-0.8	-2.46	-1.95	-8.91
P34	1,019	8.695	519	40.21	2.81	121.8	2.6	152.63	59.36	100.0	40.08	0.019	-2.04	-0.85	-0.71	-2.22	-1.82	-6.72

CE — Electrical conductivity; TDS — total dissolved solids.



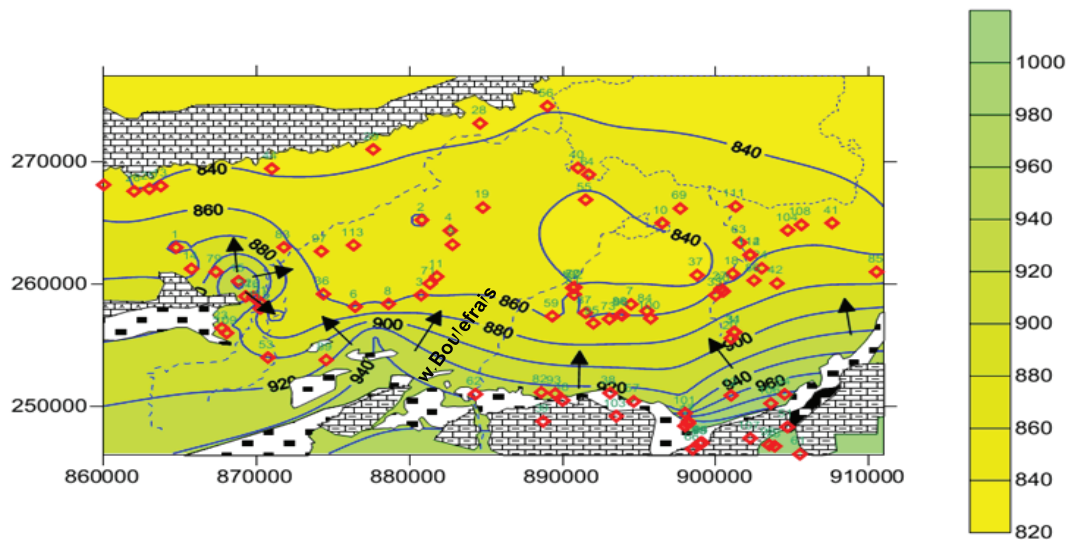


Fig. 4. Piezometric map according to Houha et al. [1].

### 3.2. Mineralization origin

To better understand the mineralization process of groundwater, we have represented major elements in function of chlorides (Fig. 5); this latter is a conserved element, not involved in water–rock interaction; characterizes the salinity origin of waters and constitutes a mixing tracer [3].

Graph  $\text{Cl}^-$  vs.  $\text{Na}^+$  shows that all the points lie below the mixing line, given that  $\text{Na}^+$  content should balance  $\text{Cl}^-$ ;  $\text{Na}^+$  deficit is explained by the phenomenon of ionic base exchange between water and the aquifer, and is reflected by  $\text{Na}^+$  adsorption and  $\text{Ca}^{2+}$  release [4,5].

The relationship between  $\text{Ca}^{2+}$  and  $\text{Cl}^-$  illustrates this by showing that the points are often above the mixing line freshwater–saltwater.

The relationship between  $\text{Mg}^{2+}$  and  $\text{Cl}^-$  shows a slight enrichment in  $\text{Mg}^{2+}$  with respect to the mixing line; this enrichment may be due to dolomite dissolution.

The relationship between  $\text{SO}_4^{2-}$  and  $\text{Cl}^-$  shows that the quasi-totality of the points lie below the mixing line freshwater–saltwater; this enrichment may be explained by evaporitic rock dissolution in aquifers, associated with contamination originating from agriculture [6,7]. In this area, the infiltration of irrigation water and rainwater loaded with soils and fertilizers is facilitated by the shallow depth of the water table and the good permeability of the soil.

The relationship between  $\text{K}^+$  and  $\text{Cl}^-$  points out that the majority of the points lie below the mixing line, except for some points that get near the line, showing that the most likely origin of  $\text{K}^+$  is pollution under the effect of NPK fertilizers and/or red clay, very abundant in the area.

### 3.3. Saturation index

Saturation index (SI) expresses the chemical balance degree between water and the mineral in the aquifer matrix, considered as a measure of dissolution and/or precipitation process concerning water–rock interaction [8]. The use of PHREEQC [9] has allowed us to calculate SI of anhydrite, aragonite, calcite, dolomite, gypsum, and halite. Generally

water–rock balance is reached when  $\text{SI} = 0$ , if  $\text{SI} > 0$ , water is supersaturated, precipitation of minerals is necessary to reach the balance. Conversely, if  $\text{SI} < 0$ , water is under saturated, the dissolution of minerals is necessary to reach the balance [10], so these minerals control the chemistry of this water. On the whole, groundwater of the study area is under-saturated with respect to gypsum, halite, and anhydrite; this suggests a probable dissolution of these minerals. In contrast, carbonate-calcium formations (calcite and aragonite) tend to be balanced (Fig. 6).

### 3.4. Identification of chemical elements origin

Groundwaters chemical process of the Tagharist Wadi basin has been studied by means of some binary diagrams of the main major elements. The first diagram has been concerned about variation of carbonate elements ( $\text{Ca}^{2+} + \text{Mg}^{2+}$  vs.  $\text{HCO}_3^-$  and  $\text{Ca}^{2+}$  vs.  $\text{HCO}_3^-$ ). These diagrams show that the points representing the different chemical analyses of sampled water are located near the line of calcite and near that of dolomite (Fig. 7); this suggests that these elements have a carbonate origin [11]. A second group of diagrams has been established by means of evaporitic elements ( $\text{Ca}^{2+}$ ,  $\text{SO}_4^{2-}$ ,  $\text{Na}^+$ , and  $\text{Cl}^-$ ). Diagram  $\text{Ca}^{2+}$  vs.  $\text{SO}_4^{2-}$  shows that the points area aligned around the slope line “1”, influenced by gypsum and/or anhydrite dissolution. Diagram  $\text{Na}^+$  vs.  $\text{Cl}^-$  shows that the points lie on the slope line “1”, indicating that halite dissolution ( $\text{Na}-\text{Cl}$ ) was the origin of these elements.

#### 3.4.1. Nitrate

Fig. 8 shows an abundance of nitrates in several water samples, which makes water unsuitable for human consumption. Indeed, 11% of the analyzed samples showed higher values than the standards permitted by the WHO (50 mg/L) with a maximum of 66.31 mg/L. On the other hand, nitrites content remains below the admissible limits. The nitrate content increases from upstream to downstream and in the same direction of groundwater flow. This increase is mainly due to the accumulation of solute toward

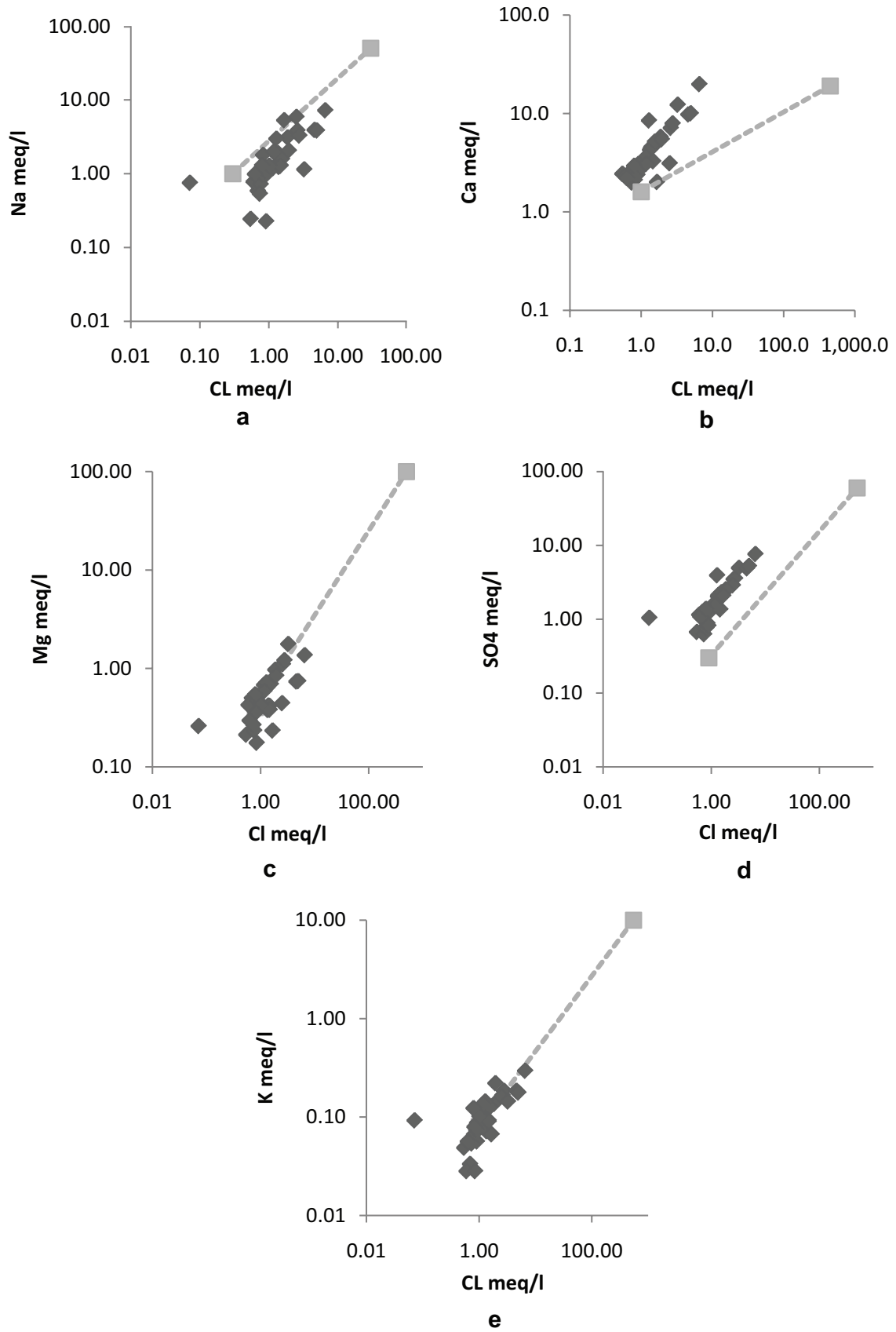


Fig. 5. Relationship between  $\text{Ca}^{2+}$ ,  $\text{Mg}^{2+}$ ,  $\text{Na}^+$ ,  $\text{SO}_4^{2-}$ ,  $\text{K}^+$ , and  $\text{Cl}^-$  of groundwater and freshwater–saltwater.

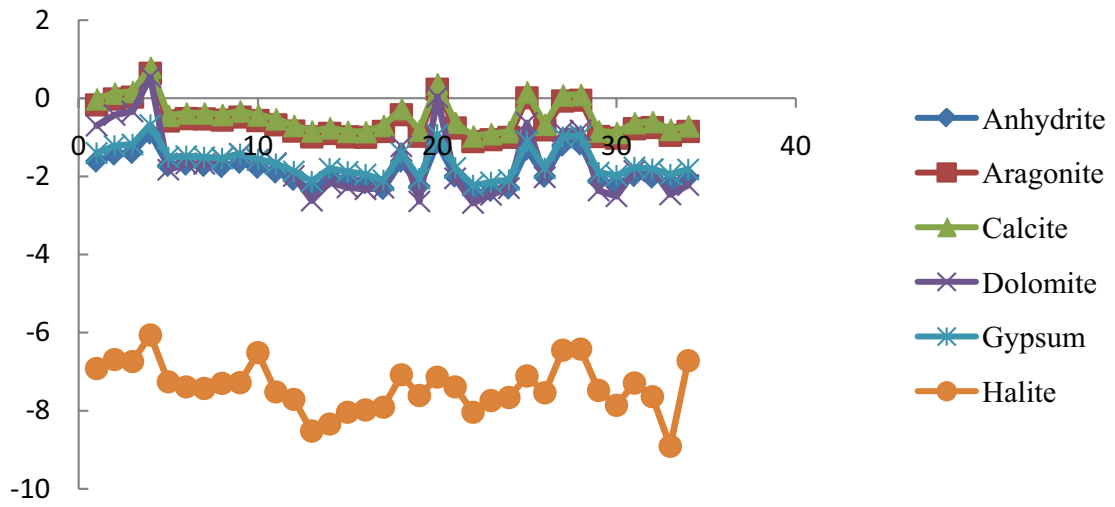


Fig. 6. Saturation index of sampled water.

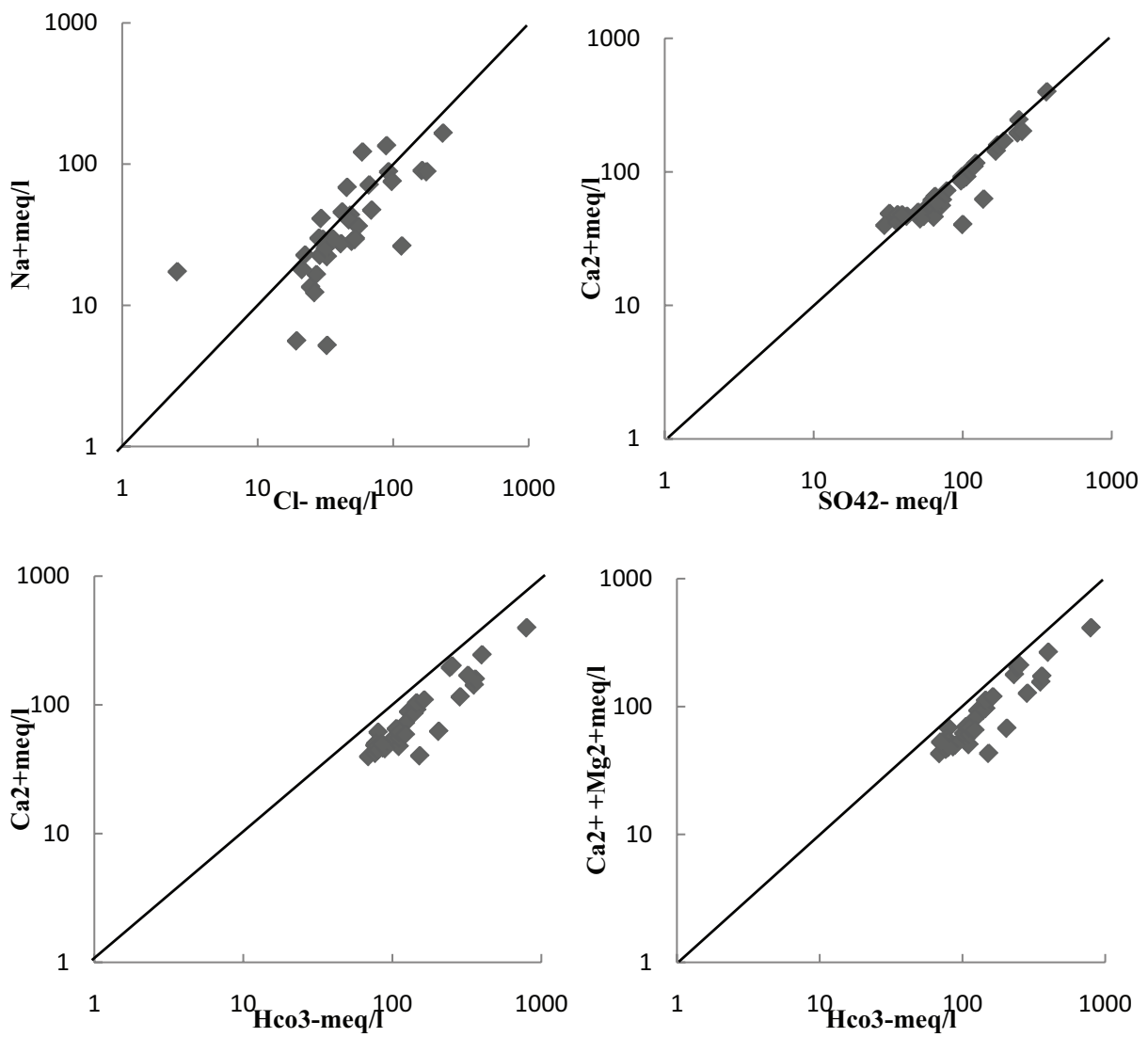


Fig. 7. Relationship between  $\text{Na}^+/\text{Cl}^-$ ,  $\text{Ca}^{2+}/\text{SO}_4^{2-}$ ,  $\text{Ca}^{2+}/\text{HCO}_3^-$ , and  $(\text{Ca}^{2+}+\text{Mg}^{2+})/\text{HCO}_3^-$ .

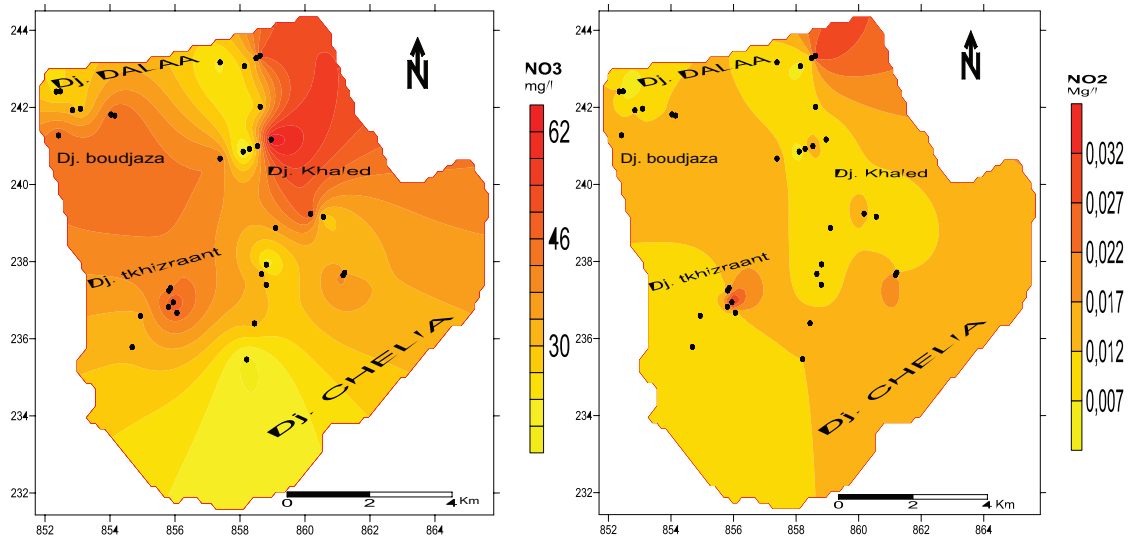


Fig. 8. Distribution of  $\text{NO}_3^-$  and  $\text{NO}_2^-$  concentrations.

the aquifer outlet. The high nitrate levels are preferentially observed in the zones at shallow water depth (<10 m) and within organic matter and nitrate-rich soils, which confirms the agricultural origin of pollution. Intensive agriculture causes leaching of nitrogen released from fertilizers and a rapid mineralization of organic soil horizons [12]. Nitrates are highly soluble in water and are transported by runoff or irrigation water, gradually penetrating into groundwater serving to supply drinking water.

3.5. Statistical multivariate analyses

The principal components analysis (PCA) was applied to discriminate the factors which mostly influence the variability and the hydrochemical classes [13,14] and then to organize them according to their order of importance.

3.6. Geochemical analyses

A statistical study by PCA has been carried out on a table of 12 variables and 34 observations. The principle of this processing has been described with more detail in the past [15,16]. The obtained results have been reported in Table 2; these analyses have allowed to draw two major factors having an expressed variances sum of 80.11% (Table 2). The analysis on factorial design F1–F2 (Figs. 9 and 10) has highlighted the general trends. In fact, factor F1 has an expressed variance of 65.08%, the most important is determined by total dissolved solids (TDS), EC,  $\text{Ca}^{2+}$ ,  $\text{Mg}^{2+}$ ,  $\text{Na}^+$ ,  $\text{K}^+$ ,  $\text{HCO}_3^-$ ,  $\text{So}_4^{2-}$ , and  $\text{Cl}^-$ . Consequently, factor F1 expresses the phenomenon of mineralization; factor F2 represents 15.03% of variance, and is characterized by  $\text{NO}_3^-$  and  $\text{NO}_2^-$ , so factor F2 expresses an organic pollution resulting from anthropogenic activity [17–22].

The space of individuals exactly reflects the localization of well 4 at the positive extremity of axis F1 that reveals a strong mineralization of its waters. On axis F2, which is a pollution axis, wells 10, 18, and 34 exhibit a high nitrate value of the order 50.51, 51.27, and 40.08 mg/L, that are opposed to well 20, that exhibits a low value of it 27.95mg/L.

Table 2  
Eigenvalues and percentage expressed by the main axes

	F1	F2
Eigenvalues	7.81	1.80
Variability (%)	65.08	15.03
Cumulative (%)	65.08	80.11

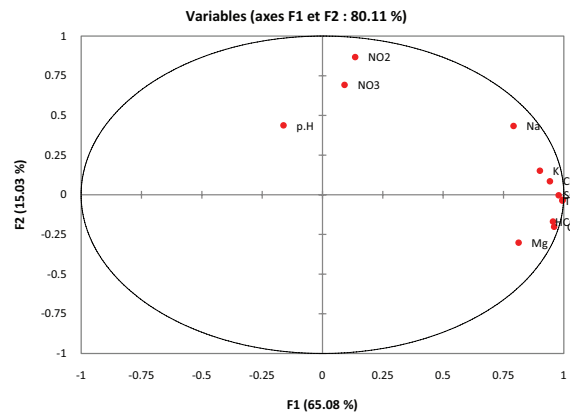


Fig. 9. Variables projection in the factorial space F1–F2.

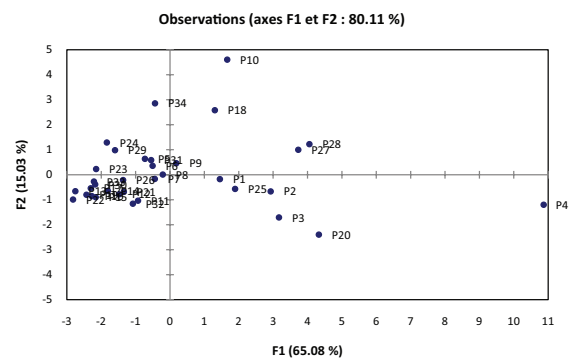


Fig. 10. Statistical projection units in the factorial space F1–F2.



#### 4. Conclusion

Hydrochemical data of well waters collected from the Tagharist Wadi basin have been used to determine the chemical process causing this mineralization. The hydrochemical study has shown that water is low to moderately mineralized. Piper diagram shows two chemical facies: bicarbonate-calcium facies (94%) and bicarbonate-sodium facies (6%).

The use of minor and major elements has allowed for the understanding of the water mineralization process. Thus, this mineralization would derive from dissolution–precipitation of the aquifer rock, evaporites, base exchange, and anthropogenic activity.

Eventually, in order to preserve the water resources from degradation, we recommend to the farmers of this region to adopt best management practices: better control of irrigation through water-saving techniques, better reasoning of mineral fertilization, as well as the frequent addition of organic amendments to the soils.

#### References

- [1] B. Houha, Etude de fonctionnement hydrogéochimique, salin et isotopique des eaux de Khenchela. Thèse de doctorat, Université D'Avignon, France, 2007, pp. 140.
- [2] A.M. Piper, A graphic procedure in geochemical interpretation of water analyses, *Trans. Am. Geophys. Union*, 25 (1994) 914–923.
- [3] M.D. Fidelibus, L. Tulipano, Regional Flow of Intruding Sea Water in the Carbonate Aquifers of Apulia (Southern Italy), *Proc. 14th Salt Water Intrusion Meeting*, Vol. 87, Rapporteur och meddelanden nr, 1996, pp. 230–241.
- [4] B. Capaccioni, M. Didero, C. Paletta, L. Idero, Saline intrusion and refreshing in a multilayer coastal aquifer in the Catania Plain (Sicily, Southern Italy): dynamics of degradation processes according to hydrochemical characteristics of groundwaters, *J. Hydrol.*, 307 (2005) 1–16.
- [5] S. Djoudi, B. Houha, The hydrochemical characterization of the upper plains aquifers: case of the plain of F'kirina Ain-Beïda, Northeastern Algeria, *Desal. Wat. Treat.*, 92 (2017) 90–97.
- [6] Y. Hamed, R. Ahmadi, A. Demdoum, S. Bouri, I. Gargouri, H. Ben Dhia, S. Al-Gamal, R. Laouar, A. Choura, Use of geochemical, isotopic, and age tracer data to develop models of groundwater flow: a case study of Gafsa mining basin-Southern Tunisia, *J. Afr. Earth Sci.*, 418 (2014) 436.
- [7] F. Touhari, M. Meddi, M. Mehaiguene, M. Razack, Hydrogeochemical assessment of the upper cheliff groundwater (North West Algeria), *Environ. Earth Sci.*, 3043 (2015) 3061.
- [8] J.F. Drever, *The Geochemistry of Natural Waters*, 3rd ed., Prentice-Hall Inc., New York, 1997, 379 pp.
- [9] L.N. Plummer, B.F. Jones, A.H. Truesdall, WATEQF; A FORTRAN IV version of WATEQ: A computer program for calculating chemical equilibrium of natural waters, Geological Survey, Water Resources Division, Washington D.C., USA, 76 (1984) 61.
- [10] S.M. Yidanaa, D. Ophoria, B. Banoeng-Yakubob, A multivariate statistical analysis of surface water chemistry data – the Ankobra Basin, Ghana, *J. Environ. Manage.*, 88 (2008) 697–707.
- [11] A. Hamad, B. Baali, R. Hadji, H. Zerrouki, H. Besser, N. Mokadem, R. Legrioui, Y. Hamed, Hydrogeochemical characterization of water mineralization in Tebessa-Kasserine karst system (Tuniso-Algerian Transboundary basin), *Euro-Mediterr. J. Environ. Integr.*, 3 (2018) 7.
- [12] A. Fernández-Cirelli, J.L. Arumí, D. Rivera, P.W. Boochs, Environmental effects of irrigation in arid and semi-arid regions, *Chil. J. Agric. Res.*, 69 (2009) 27–40.
- [13] V.P. Evangelou, J. Lumbanraja, Ammonium-potassium-calcium exchange on vermiculite and hydroxyl-aluminium vermiculite, *Soil Sci. Soc. Am. J.*, 66 (2002) 445–455.
- [14] A. Melloul, M. Collin, The principal component statistical method as a complementary approach to geochemical methods in water quality factor identification: application to the coastal plain aquifer of Israel, *J. Hydrol.*, 140 (1992) 49–73.
- [15] T. Foucart, *Analyse Factorielle*, Programmation sur micro-ordinateur, Masson, Ed., France, 1982.
- [16] A. Mangin, Contribution à l'étude hydrodynamique des aquifères karstiques, Concepts méthodologiques adoptés, Systèmes karstiques étudiés, *Ann. Spéléol.*, 29 (1974) 495–601.
- [17] Y. Hamed, S. Awad, A. Ben Sâad, Nitrate contamination in groundwater in the Sidi Aïch-Gafsa Oasis region, Southern Tunisia, *J. Environ. Earth Sci.*, 70 (2013) 2335–2348.
- [18] Y. Hamed, R. Ahmadi, A. Demdoum, I. Gargouri, R. Hadji, S. Bouri, H. Ben Dhia, S. Al Gamal, R. Laouar, A. Choura, Use of geochemical, isotopic, and age tracer data to develop models of groundwater flow: a case study of Gafsa mining basin-Southern Tunisia, *J. Afr. Earth Sci.*, 100 (2014) 418–436.
- [19] Y. Ayadi, N. Mokaddem, B. Redhaounia, Y. Hamed, The Impact of Climate Change on Future Nitrate Concentration in Groundwater of Bled Abida Basin El Kef Region (NW Tunisia), *Colloque International sur l'hydrogéologie et la géothermie*, le 11–12 November, Guelma, Algérie, 2014.
- [20] Y. Ayadi, B. Redhaounia, Y. Hamed, Groundwater Contamination in the Aquifer System of El Houdh-Bled Abida Basin (North western Tunisia), *International Symposium on Water Pollution and Environmental Impacts in the Mediterranean Basin*, le 23–27 November, Sousse, Tunisie, 2014.
- [21] N. Mokadem, H. Younes, M. Hfaïd, H. Ben Dhia, Hydrogeochemical and isotope evidence of groundwater evolution in El Guettar Oasis area, Southwest Tunisia, *Carbonates Evaporites*, 30 (2015) 417–437.
- [22] N. Mokadem, A. Demdoum, Y. Hamed, S. Bouri, R. Hadji, A. Boyce, R. Laouar, A. Saad, Hydrogeochemical and stable isotope data of groundwater of a multi-aquifer system: Northern Gafsa basin (Central Tunisia), *J. Afr. Earth Sci.*, 114 (2016) 174–191.